ACS APPLIED MATERIALS & INTERFACES

Research Article

www.acsami.org

High-Mobility Pyrene-Based Semiconductor for Organic Thin-Film Transistors

Hyunduck Cho,[†,‡] Sunyoung Lee,[†,§] Nam Sung Cho,[⊥] Ghassan E. Jabbour,[∥] Jeonghun Kwak,[△] Do-Hoon Hwang,*[,#] and Changhee Lee*[,‡]

[‡]Department of Electrical and Computer Engineering, Inter-university Semiconductor Research Center, Seoul National University, Seoul 151-744, Korea

[§]Department of Applied Chemistry, Kumoh National Institute of Technology, Gumi 730-701, Korea

[⊥]Convergence Components & Materials Laboratory, Electronics and Telecommunications Research Institute (ETRI), 161 Gajeon-dong, Yuseong-gu, Daejeon 305-350, Korea

[∥]Flexible Display Center and School of Materials, Arizona State University, 7700 S. River Parkway, Tempe, Arizona 85284, United States

[△]Department of Electronic Engineering, Dong-A University, Busan 604-714, Korea

[#]Department of Chemistry, and Chemistry Institute for Functional Materials, Pusan National University, Busan 609-735, Korea

Supporting Information

ABSTRACT: Numerous conjugated oligoacenes and polythiophenes are being heavily studied in the search for high-mobility organic semiconductors. Although many researchers have designed fused aromatic compounds as organic semiconductors for organic thin-film transistors (OTFTs), pyrene-based organic semiconductors with high mobilities and on−off current ratios have not yet been reported. Here, we introduce a new pyrene-based p-type organic semiconductor showing liquid crystal behavior. The thin film characteristics of this material are investigated by varying the substrate temperature during the deposition and the gate dielectric condition using the surface modification with a self-assembled monolayer, and systematically studied in correlation with the performances of transistor devices with this compound. OTFT fabricated under the optimum deposition conditions of this compound, namely, 1,6-bis(5′-octyl-2,2′-bithiophen-5-yl)pyrene (BOBTP) shows a high-performance transistor behavior with a field-effect mobility of 2.1 $cm^2 V^{-1} s^{-1}$ and an on−off current ratio of 7.6×10^6 and enhanced long-term stability compared to the pentacene thin-film transistor.

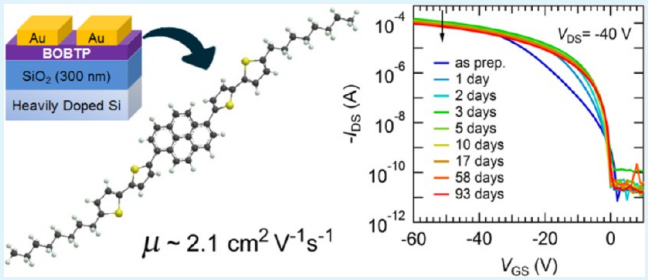

KEYWORDS: *pyrene, liquid crystals, organic semiconductors, thin films, field-effect transistors*

1. INTRODUCTION

In the near future, organic thin-film transistors (OTFTs) are expected to create a new market for flexible and printed electronics that will have the advantages of low manufacturing costs and large-area fabrication and include device applications such as radio frequency identification (RFID) tags, sensors, drivers for electronic paper displays, and flexible displays.[1−5] Much effort on synthesis has been devoted to developing superior organic semiconductors with high charge carrier mobilities when incorporated into OTFTs. Numerous conjugated oligoacenes, thienoacene, and polythiophenes have been heavily studied in the search for high-mobility organic semiconductors.[5,6] Among them, pentacene is one of the most promising materials, exhibiting some of the best performances with a field-effect mobility of 3 $cm^2 V^{-1} s^{-1}$ in vacuum-deposited devices.[7] Although many researchers have designed fused aromatic compounds as organic semiconductors for OTFTs, pyrene-based organic semiconductors with high mobilities and on−off current ratios have not yet been reported.

The pyrene core is a widely used probe due to its high fluorescent efficiency and excimer formation,[8] and a number of pyrene derivatives have recently been reported to show liquid crystal (LC) behavior.[9] Although the reported field-effect mobilities of pyrene derivatives in OTFTs are poor,[10] we expected that pyrene-based semiconductors had high mobilities because of the properties provided by their highly ordered crystalline structure and the increase in charge transport due to their fused-ring aromatic structure.[11] To increase the performance of OTFTs with respect to properties such as field-effect

Received: February 8, 2013
Accepted: April 5, 2013
Published: April 5, 2013

Scheme 1. Synthesis of 1,6-Bis(5-octyl-2,2′-bithiophen-5-yl)pyrene

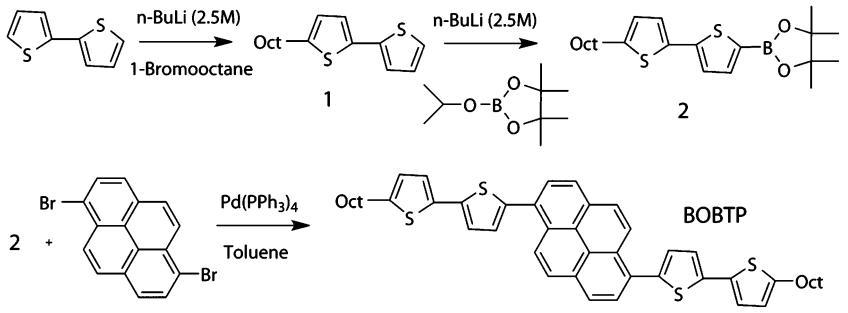

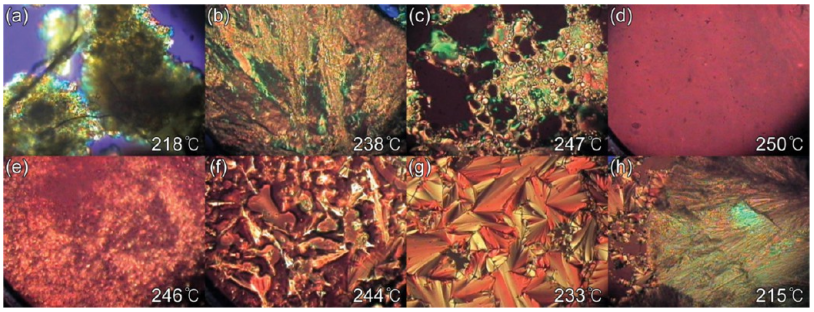

Figure 1. Polarized optical microscopic images of BOBTP upon (a–d) heating from 218 to 250 °C and (e–h) cooling from 246 to 215 °C (magnification of 250×). Upon cooling, the nematic phases were found at (f) 244 °C and the smectic phases at (g) 233 °C.

mobility and on–off current ratio, it is crucial that the architecture of the organic semiconductor molecules is controlled at the molecular level. Substitution at the 1,6-position on the pyrene backbone is expected to give the most extended π-conjugation and the highest degree of planarity due to the retention of linearity and limited steric hindrance. Ando et al. reported a p-type organic semiconductor produced by introducing electron-donating thiophenes as terminal groups into an anthracene unit.[12] The addition of alkyl side-chains at both ends is known to introduce self-assembly properties, which lead to an improvement of the structural ordering of molecules and result in a high mobility.[13,14] Further observation suggested that the addition of alkyl groups is a more effective way to improve mobility than the extension of π-conjugation.[15]

In this paper, we report the synthesis and characterization of a new pyrene-based p-type semiconducting compound, 1,6-bis(5′-octyl-2,2′-bithiophen-5-yl)pyrene (BOBTP), prepared by adding alkyl-thiophene units to a pyrene core. The designed molecule is composed of small fused aromatics and is expected to have a linear structure with a high degree of conjugation along the backbone of the molecule and result in efficient carrier transport. The field-effect mobility (μ), threshold voltage (V_{th}), on–off current ratio ($I_{on/off}$) and subthreshold slope (SS) were investigated to evaluate the performance of OTFTs fabricated using BOBTP thin films. The BOBTP thin-film transistor (TFT) showed good performance with high hole mobility up to 2.1 $cm^2\ V^{-1}\ s^{-1}$ and $I_{on/off}$ of 7.6×10^6 in ambient air, and also had good long-term stability in ambient air over 4 months.

2. RESULTS AND DISCUSSION

2.1. Synthesis and Characterization. The synthetic route for producing BOBTP is given in Scheme 1. BOBTP was synthesized by a one-step Suzuki coupling reaction using 5-octyl-5′-(4,4,5,5-tetramethyl-1,3,2-dioxaborolanyl)-2,2′-bithiophene and 1,6-dibromopyrene with 2 M aqueous K_2CO_3 and $Pd(PPh_3)_4$ as catalyst. The crude product was chromatographed on Florisil with hot chloroform. The BOBTP was then purified by recrystallization using methanol and washed with hexane, chloroform, and methanol using a Soxhlet extractor. The final products were verified by NMR, mass spectrometry, and elemental analysis (85% yield). Details of the synthesis of materials are described in the Supporting Information.

The UV–vis absorption spectrum of a dilute solution of BOBTP in chloroform shows two distinct peaks at 322 and 410 nm (see Figure S3 in the Supporting Information). The absorption spectrum in the solid-state thin film shows a hypsochromic shift compared to that of the solution, with the peaks moving to 331 and 362 nm, respectively. This phenomenon can be explained by H-aggregation, which is usually related to excitonic coupling between adjacent molecules in a close-packed structure.[16] Rigid backbone molecules with completely coplanar π surfaces induced by a flat pyrene connected to twisted bithienyl rings are also expected to promote π–π stacking.[17] This enables intermolecular electronic coupling and more efficient H-aggregation due to the highly regular face-to-face stacking of coplanar molecules.[18] The optical band gap was determined by extrapolating the absorption edge using the empirical equation ($E_g = 1240/\lambda_{onset}$),[19] which was measured to be 2.52 eV.

The highest occupied molecular orbital (HOMO) energy level of this compound was found at 5.05 eV by photoelectron spectroscopy (see Figure S4 in the Supporting Information). Also, the electrochemically estimated HOMO level using cyclic voltammetric (CV) measurement exhibited the same energy level (see Figure S5 in the Supporting Information). The HOMO energy level matches the work function of Au electrodes and ensures holes inject effectively from the Au electrode to the active layer in an OTFT.

The thermal behavior of BOBTP was evaluated by the differential scanning calorimetry (DSC) (see Figure S6 in the

Supporting Information). The DSC thermogram exhibits two endotherms at 223 and 243 °C, which correspond to the melting and isotropization temperature, respectively. Therefore, BOBTP was expected to have a mesophase between the two endotherms. As shown in Figure 1, the LC phase was clearly confirmed at 233 °C upon cooling using a polarized optical microscope (POM) with a hot stage. From the POM experiment, two DSC endotherms could be interpreted as the crystal to LC transition at 223 °C and LC-to-isotropic transition at 243 °C. The LC behavior is known to be favorable for charge transport in organic semiconductors because of the molecular ordering during the LC phase.[20] From the thermo-gravimetric analysis (TGA) in a nitrogen atmosphere, BOBTP showed good thermal stability with losing 1% of its weight upon heating to 408 °C (see Figure S4 in the Supporting Information), which surpass the thermal stability of pentacene with losing 1% of the mass at 323 °C.[21]

2.2. Thin-Film Morphology. Polycrystalline structures were observed from atomic force microscope (AFM) images of BOBTP thin films. BOBTP was deposited on the SiO_2 and octadecyltrichlorosilane (OTS) self-assembled monolayer (SAM) modified SiO_2 substrates at the various film deposition temperature (T_d) of room temperature (RT, 25 °C), 90, 120, and 150 °C. As can be seen in Figure 2, the average grain size increased as T_d was increased from room temperature to 120 °C. At T_d = RT, the average grain sizes on bare and OTS-treated SiO_2 were 83 and 290 nm, respectively (Figure 2a, b).

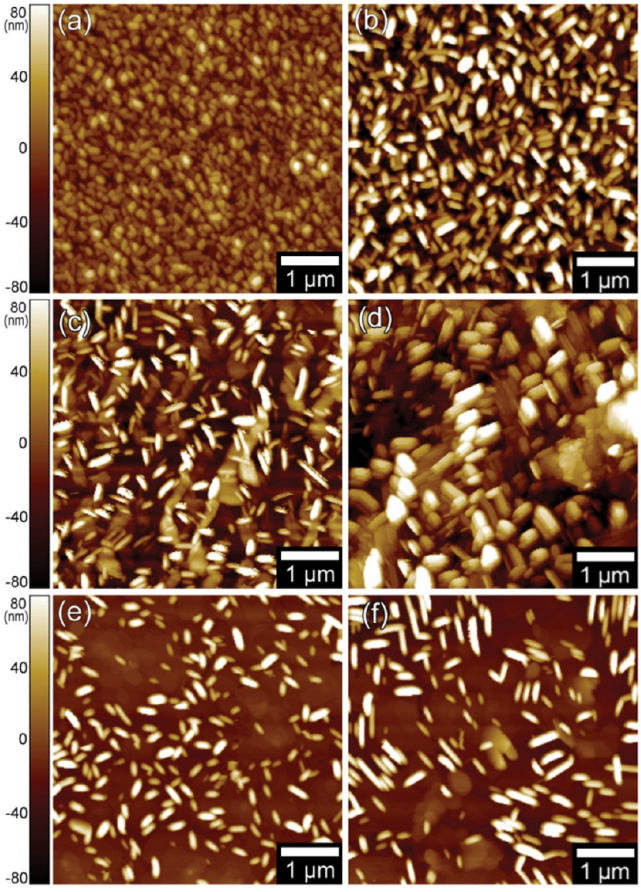

Figure 2. AFM images of BOBTP layers at various substrate deposition temperatures (T_d) of (a, b) 25, (c, d) 120, and (e, f) 150 °C on bare SiO_2 (left) and OTS-treated SiO_2 substrates (right).

At T_d = 120 °C, rodlike grains with an average length of 290 nm and average width of 100 nm were observed in the BOBTP film on bare SiO_2 (Figure 2c). The grains on the OTS-treated SiO_2 surface were larger than those on the bare SiO_2 surface, of which the average grain length and width were 350 and 290 nm, respectively (Figure 2d). Grain sizes of vacuum-deposited pentacene film on OTS/SiO_2 are typically smaller than those on bare SiO_2, probably due to the rough surface produced after the OTS treatment.[22] However, the larger grains of this compound on OTS/SiO_2 were possibly influenced more by the lower energy of the OTS-SAM dielectric surface than by the roughness of the surface. As T_d was further increased to 150 °C, the size of the rodlike grains was reduced, and AFM images show the lower density of the grains (Figure 2e, f).

The molecular ordering in the thin film was investigated by X-ray diffraction (XRD) as shown in Figure 3. The first peak in

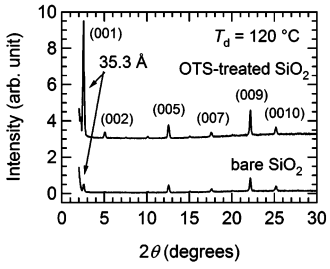

Figure 3. X-ray diffraction patterns of 100-nm thick BOBTP films on bare and OTS-treated SiO_2 surfaces at T_d = 120 °C.

the XRD patterns at 2θ = 2.5° corresponds to a d-spacing of 35.3 Å. Up to 10 peaks could be found. The interlayer spacing of 35.3 Å is less than the molecular length of 45 Å calculated from the distance between the edge hydrogen atoms. Only (00l) planes were observed in the thin film XRD patterns, whereas the other planes were shown in the powder XRD pattern (see Figure S8 in the Supporting Information). The absence of other planes indicates that the π-stacking direction is almost aligned with the direction of carrier movement in the channel.[23] As a result of this structure, the devices could show high field-effect mobility. The peak intensities for the thin film on OTS/SiO_2 surface were higher than for the thin film on bare SiO_2 surface, indicating higher crystallinity of the BOBTP thin film on OTS/SiO_2 than on bare SiO_2.

2.3. OTFT Performance and Air Stability. To investigate OTFT performance, we fabricated top-contact, bottom-gate OTFTs using vacuum-deposited BOBTP at various substrate temperatures and characterized then in the air or a nitrogen atmosphere. For the comparison, we also fabricated pentacene OTFTs with the same structure at T_d = 70 °C at the same time. The transistor key parameters (μ, V_{th}, $I_{on/off}$, SS) in various conditions were extracted from the transfer characteristics in the saturation regime and are summarized in Table 1. Panels a and b in Figure 4 show the transfer characteristics of BOBTP OTFTs on bare SiO_2 and OTS-treated SiO_2 at T_d of RT, 90, 120, and 150 °C. The mobilities of them increased as T_d was increased from RT to 120 °C. The highest mobility in the BOBTP TFT on OTS/SiO_2 at T_d = 120 °C was measured as 2.1 $cm^2\ V^{-1}\ s^{-1}$ in the air condition, which is about 8 times higher than that of the pentacene device (0.26 $cm^2\ V^{-1}\ s^{-1}$). At various T_d, the μ values of BOBTP OTFTs on OTS/SiO_2 surface were higher than those on bare SiO_2. The output characteristics of BOBTP OTFT at 120 °C in panels c and d in

Table 1. Key Parameters of BOBTP and Pentacene OTFTs on Bare SiO_2 and OTS-Treated SiO_2 Substrates at Various Conditions[a]

compd	dielectric surface	T_d (°C)	μ ($cm^2\ V^{-1}s^{-1}$)	V_{th} (V)	I_{on}/I_{off} (A/A)	SS (V dec^{-1})
BOBTP[b]	SiO_2	25 (RT)	0.41	−10.1	1.2×10^6	1.6
		90	0.67	−22.7	4.8×10^6	1.0
		120	0.65	−11.4	4.6×10^6	0.95
		150	0.47	−10.7	1.3×10^6	1.6
	OTS/SiO_2	25 (RT)	1.4	−15.8	4.1×10^6	1.6
		90	1.5	−19.6	2.4×10^7	0.81
		120	1.9	−19.9	4.8×10^6	1.1
		150	0.58	−10.0	5.6×10^6	1.4
pentacene[b]	OTS/SiO_2	70	0.25	−9.6	1.0×10^5	0.90
BOBTP[c]	OTS/SiO_2	120	2.1	−17.5	7.6×10^6	0.94
pentacene[c]	OTS/SiO_2	70	0.26	−7.7	3.9×10^6	1.0

[a]TFT parameters were extracted from the devices of W = 1000 μm and L = 110 μm. Electrical characteristics were measured in a. [b]Nitrogen atmosphere. [c]Ambient air.

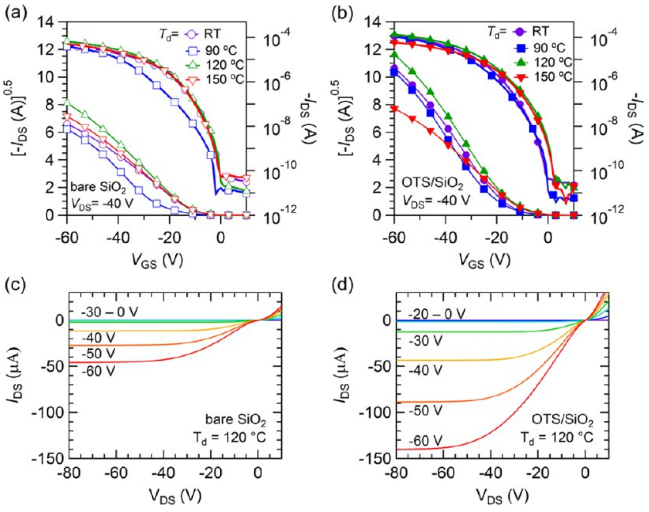

Figure 4. Transfer characteristics of BOBTP OTFTs on (a) bare SiO_2 and (b) OTS-treated SiO_2 substrates at various substrate deposition temperatures (T_d), and the output curves (c, d) at T_d = 120 °C on each substrate under the nitrogen condition.

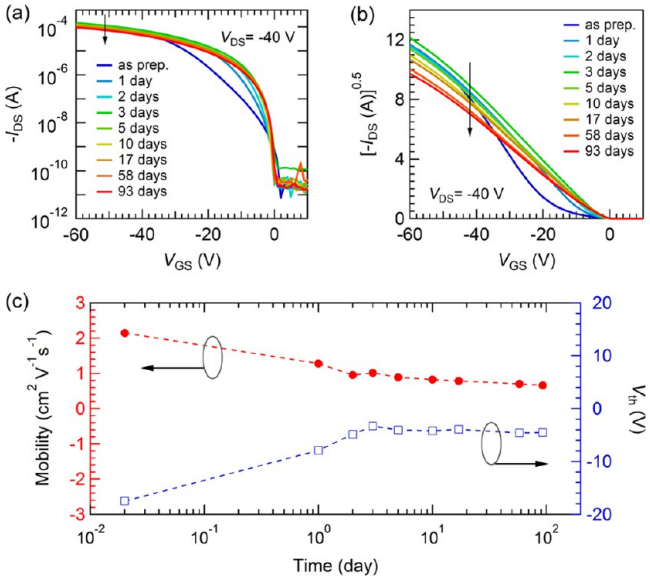

Figure 5. Air stability of BOBTP was measured in terms of (a) the transfer characteristics and (b) $[-I_{DS}]^{0.5} - V_{GS}$ curves under ambient air condition. (c) Plot of the mobility and threshold voltage changes for 3 months. All the data were obtained from the devices with W/L = 1000/110 μm.

Figure 4c clearly show the difference of the drain current between bare and OTS-treated SiO_2. These results agree with the above AFM and XRD data of BOBTP thin films. Generally, the mobility of OTFTs increases as grain size increases because of the reduced potential barriers between grains.[24] The mobility, however, decreased significantly at T_d = 150 °C. This was probably due to less dense packing of grains and an increase in unoccupied volume between grains,[25,26] as shown in the corresponding AFM images (Figure 3e, f). For the BOBTP TFTs, $I_{on/off}$ of 1×10^6 to 1×10^7 were observed, which were similar or higher than typical pentacene devices.

Shelf-lifetime of BOBTP OTFTs had been examined for about 3 months by keeping them in ambient air at room temperature. The transfer characteristics and $[-I_{DS}]^{0.5}-V_{GS}$ curves for 93 days are plotted in panels a and b in Figure 5, respectively, and the time dependent μ and V_{th} values extracted from these curves are shown in Figure 5c. At the early stage, transistor charactersitics of BOBTP changed significantly. For example, μ decreased from 2.1 to 1.0 $cm^2\ V^{-1}\ s^{-1}$ and V_{th} increased from −17.5 V to −3.3 V for 3 days. These changes for 3 days in μ and V_{th}, nevertheless, did not influence on the values of I_{DS}. After going through the early stage of changes, the devices retained its mobility and threshold voltage for the rest time in the shelf. In case of pentacene OTFT, there was no significant degradation in the early stage, but the mobility and drain current were decreased more and more as time goes on. At day 93, the mobility of BOBTP was decreased by about 34% while that of pentacene was decreased by about 57% to the values at day 1 (see Figure S9 in the Supporting Information). We, therefore, think that BOBTP OTFTs are much stable than pentacene OTFTs.

3. CONCLUSIONS

In summary, we have demonstrated the high performance of a p-type OTFT using a new organic semiconductor possessing LC nature based on pyrene and thiophene, BOBTP. The charcteristics of the BOBTP thin films were studied in correlation with the performance of transistor devices by varying the deposition temperature and the surface hydrophobicity of gate dielectric. The OTFT using BOBTP showed a field-effect mobility as high as 2.1 $cm^2\ V^{-1}\ s^{-1}$ and an on−off

current ratio 7.6×10^6 under the optimized condition. In addition, BOBTP TFT showed better air stability than that of pentacene TFT for 3 months. These results indicate that this pyrene-based compound is a good organic semiconductor candidate for organic electronics applications.

4. EXPERIMENTAL SECTION

Materials and Measurements. 2,2′-Bithiophene, 1-bromooctane, n-butyllithium (2.5 M in hexane), 2-isopropoxy-4,4,5,5-tetramethyl-1,3,2-dioxaborolane, anhydrous toluene, and Aliquat 336 were obtained from Aldrich Chemical Co. HPLC-grade chloroform, hexane, methanol, acetone, and THF were purchased from J.T. Baker Chemical Co, and THF was dried over Na/benzophenone ketyl and freshly distilled prior to use. Tetrakis(triphenylphosphine)palladium was purchased from Strem Chemical Co, and the other reagents and solvents were purchased commercially and used without further purification. All reactions were carried out in an argon or nitrogen atmosphere with anhydrous solvents. The UV−vis spectra were recorded on a Shimadzu UV-3600/vis spectrometer. Cyclic voltammetry (CV) was performed on an SP-150 potentiostat by Neoscience with a three-electrode cell in an electrolyte solution of 0.1 M tetrabutylammonium tetrafluoroborate ($TBABF_4$) in anhydrous acetonitrile at room temperature under nitrogen gas with a scan rate of 100 mV s^{-1}. The counter electrode was a Pt wire, and the reference electrode was an $Ag/AgNO_3$ (0.01 M) electrode. A film of material was coated onto the Pt wire electrode by dipping the electrode into a solution of the material and used as the working electrode. The HOMO energy level was determined by photoelectron spectroscopy (Hitachi High Tech. AC-2) with a UV light intensity of 10 nW. Thermal gravimetric analysis (TGA) was carried out using a TA Instruments TGA Q500 instrument (heating rate of 10 °C min^{-1}), and differential scanning calorimetry (DSC) measurements were performed with a NETZSCH DSC 200F3 under a nitrogen atmosphere (scanning rate of 10 °C min^{-1}). A polarized optical microscope (Jenapol, Zeiss) equipped with an FP82 hot stage (Mettler) was used to observe the thermal behavior of the material. The sample was placed on a glass slide, covered with a glass coverslip and heated on the hot stage at 10 °C/min and cooled at 5 °C min^{-1}. Thin-film X-ray diffraction (XRD) patterns were obtained using a Bruker D8 advance X-ray diffractometer with a Cu Kα1 source (λ = 1.5406 Å), operating at 40 kV and 40 mA. The surface morphologies were characterized using atomic force microscopy (AFM, PSIA XE-100) using a noncontact mode.

OTFT Fabrication and Characterization. OTFTs with top-contact bottom-gate geometry were prepared on heavily doped Si substrates used as common gate electrodes with thermally grown 300 nm-thick SiO_2 layers as gate dielectrics. The unit area capacitance of the gate dielectric was 11.8 nF cm^{-2}. For OTS treatment on dielectric surfaces, the SiO_2/Si substrates were UV-ozone-treated for 10 min and rinsed by deionized water. The cleaned substrates were immersed in a 2 mmol solution of OTS in hexadecane for 16 h. Then, the substrates were sonicated in chloroform, isopropyl alcohol, and deionized water for 10 min each and dried at 120 °C in air for 5 min. A 100-nm-thick BOBTP film was deposited at a pressure of 10^{-6} Torr and a rate of 0.3−0.4 Å s^{-1}. A 50-nm-thick Au film used as source and drain electrodes was also deposited through a shadow mask at a rate of 1 Å s^{-1}. The prepared OTFTs had channel widths (W) of 1000 μm and channel lengths (L) of 110 μm. Electrical characterizations of OTFTs were performed using a semiconductor parameter analyzer (HP 4155C) in a nitrogen atmosphere or ambient air.

■ ASSOCIATED CONTENT

Supporting Information

Details of synthesis and instruments, ^1H NMR and ^{13}C NMR spectra, UV−vis absorption spectra, photoemission spectrum, CV, DSC and TGA curves, and XRD pattern of BOBTP powder, and air-stability of pentacene OTFTs. This information is available free of charge via the Internet at http://pubs.acs.org/.

■ AUTHOR INFORMATION

Corresponding Author

*E-mail: chlee7@snu.ac.kr (C.L.); dohoonhwang@pusan.ac.kr (D.H.H.).

Author Contributions

†H. Cho and S. Lee contributed equally to this work.

Notes

The authors declare no competing financial interest.

■ ACKNOWLEDGMENTS

This work was supported by the Industrial Strategic Technology Development Program (KI002104, Development of Fundamental Technologies for Flexible Combined-Function Organic Electronic Device) funded by the Ministry of Knowledge Economy (MKE, Korea) and a grant (2012055225) from the Center for Advanced Soft Electronics under the Global Frontier Research Program of the Ministry of Education, Science and Technology, Korea.

■ REFERENCES

(1) (a) Ong, B. S.; Wu, Y.; Liu, P.; Gardner, S. *J. Am. Chem. Soc.* **2004**, *126*, 3378. (b) Ong, B. S.; Wu, Y.; Liu, P.; Gardner, S. *Adv. Mater.* **2005**, *17*, 1141. (c) Li, Y.; Wu, Y.; Liu, P.; Birau, M.; Pan, H.; Ong, B. S. *Adv. Mater.* **2006**, *18*, 3029.

(2) (a) Noh, Y.-Y.; Kim, D.-Y.; Yoshida, Y.; Yase, K.; Jung, B.-J.; Lim, E.; Shim, H.-K. *Appl. Phys. Lett.* **2005**, *86*, 043501. (b) Baeg, K.-J.; Noh, Y.-Y.; Ghim, J.; Kang, S.-J.; Lee, H.; Kim, D.-Y. *Adv. Mater.* **2006**, *18*, 3179. (c) Noh, Y.-Y.; Zhao, N.; Caironi, M.; Sirringhaus, H. *Nat. Nanotechnol.* **2007**, *2*, 784.

(3) (a) Dimitrakopoulos, C. D.; Malenfant, P. R. L. *Adv. Mater.* **2002**, *14*, 99. (b) McCulloch, I.; Heeney, M.; Bailey, C.; Genevicius, K.; Macdonald, I.; Shkunov, M.; Sparrowe, D.; Tierney, S.; Wagner, R.; Zhang, W.; Chabinyc, M. L.; Kline, R. J.; McGehee, M. D.; Toney, M. F. *Nat. Mater.* **2006**, *5*, 328. (c) Takimiya, K.; Kunugi, Y.; Konda, Y.; Ebata, H.; Toyoshima, Y.; Otsubo, T. *J. Am. Chem. Soc.* **2006**, *128*, 3044.

(4) (a) Murphy, A. R.; J. Fréchet, J. M. *Chem. Rev.* **2007**, *107*, 1066. (b) Katz, H. E. *Chem. Mater.* **2004**, *16*, 4748. (c) Facchetti, A. *Mater. Today* **2007**, *10*, 28.

(5) (a) Meng, Q.; Dong, H.; Hu, W.; Zhu, D. *J. Mater. Chem.* **2011**, *21*, 11708. (b) Yamamoto, T.; Nishimura, T.; Mori, T.; Miyazaki, E.; Osaka, I.; Takimiya, K. *Org. Lett.* **2012**, *14*, 4914. (c) Li, J.; Zhao, Y.; Tan, H. S.; Guo, Y.; Di, C.-A.; Yu, G.; Liu, Y.; Lin, M.; Lim, S. H.; Zhou, Y.; Su, H.; Ong, B. S. *Sci. Rep.* **2012**, *2*, 754.

(6) (a) Youn, J.; Chen, M.-C.; Liang, Y.-J.; Huang, H.; Ortiz, R. P.; Kim, C.; Stern, C.; Hu, T.-S.; Chen, L.-H.; Yan, J.-Y.; Facchetti, A.; Marks, T. J. *Chem. Mater.* **2010**, *22*, 5031. (b) Youn, J.; Huang, P.-Y.; Huang, Y.-W.; Chen, M.-C.; Lin, Y.-J.; Huang, H.; Ortiz, R. P.; Stern, C.; Chung, M.-C.; Feng, C.-Y.; Chen, L.-H.; Facchetti, A.; Marks, T. J. *Adv. Funct. Mater.* **2012**, *22*, 48. (c) Huang, P.-Y.; Chen, L.-H.; Kim, C.; Chang, H.-C.; Liang, Y.-J.; Feng, C.-Y.; Yeh, C.-M.; Ho, J.-C.; Lee, C.-C.; Chen, M.-C. *ACS Appl. Mater. Interfaces* **2012**, *4*, 6992.

(7) Klauk, H.; Halik, M.; Zschieschang, U.; Schmid, G.; Radlik, W.; Weber, W. *J. Appl. Phys.* **2002**, *92*, 5259.

(8) (a) Cheng, C.-H.; Shih, H.-T.; Wu, K.-C.; US Patent 6861163, 2005. (b) Tao, S.; Peng, Z.; Zhang, X.; Wang, P.; Lee, C.-S.; Lee, S.-T. *Adv. Funct. Mater.* **2005**, *15*, 1716. (c) Tang, C.; Liu, F.; Xia, Y.-J.; Xie, L.-H.; Wei, A.; Li, S.-B.; Fan, Q.-L.; Huang, W. *J. Mater. Chem.* **2006**, *16*, 4074. (d) Mikroyannidis, J. A.; Fenenko, L.; Adachi, C. *J. Phys. Chem. B* **2006**, *110*, 20317. (e) Lo, M. Y.; Zhen, C.; Lauters, M.; Jabbour, G. E.; Sellinger, A. *J. Am. Chem. Soc.* **2007**, *129*, 5808.

(9) Sagara, Y.; Kato, T. *Angew. Chem., Int. Ed.* **2008**, *47*, 5175.

(10) (a) Zhang, H.; Wang, Y.; Shao, K.; Liu, Y.; Chen, S.; Qiu, W.; Sun, X.; Qi, T.; Ma, Y.; Yu, G.; Su, Z.; Zhu, D. *Chem. Commun.* **2006**, 755. (b) Wang, Y.; Wang, H.; Liu, Y.; Di, C.-A.; Sun, Y.; Wu, W.; Yu, G.; Zhang, D.; Zhu, D. *J. Am. Chem. Soc.* **2006**, *128*, 13058.
(11) Ashizawa, M.; Yamada, K.; Fukaya, A.; Kato, R.; Hara, K.; Takeya, J. *Chem. Mater.* **2008**, *20*, 4883.
(12) Ando, S.; Nishida, J.-I.; Fujiwara, E.; Tada, H.; Inoue, Y.; Tokito, S.; Yamashita, Y. *Chem. Mater.* **2005**, *17*, 1261.
(13) Garnier, F.; Yassar, A.; Hajlaoui, R.; Horowitz, G.; Deloffre, F.; Servet, B.; Ries, S.; Alnot, P. *J. Am. Chem. Soc.* **1993**, *115*, 8716.
(14) Meng, H.; Sun, F.; Goldfinger, M. B.; Jaycox, G. D.; Li, Z.; Marshall, W. J.; Blackman, G. S. *J. Am. Chem. Soc.* **2005**, *127*, 2406.
(15) (a) Ito, K.; Suzuki, T.; Sakamoto, Y.; Kubota, D.; Inoue, Y.; Sato, F.; Tokito, S. *Angew. Chem., Int. Ed.* **2003**, *42*, 1159. (b) Inoue, Y.; Tokito, S.; Ito, K.; Suzuki, T. *J. Appl. Phys.* **2004**, *95*, 5795.
(16) Drolet, N.; Morin, J.-F.; Leclerc, N.; Wakim, S.; Tao, Y.; Leclerc, M. *Adv. Funct. Mater.* **2005**, *15*, 1671.
(17) Balakrishnan, K.; Datar, A.; Zhang, W.; Yang, X.; Naddo, T.; Huang, J.; Zuo, J.; Yen, M.; Moore, J. S.; Zang, L. *J. Am. Chem. Soc.* **2006**, *128*, 6576.
(18) Fang, Q.; Wang, F.; Zhao, H.; Liu, X.; Tu, R.; Wang, D.; Zhang, Z. *J. Phys. Chem. B* **2008**, *112*, 2837.
(19) Kong, H.; Chung, D. S.; Kang, I.-N.; Park, J.-H.; Park, M.-J.; Jung, I. H.; Park, C. E.; Shim, H.-K. *J. Mater. Chem.* **2009**, *19*, 3490.
(20) (a) Sirringhaus, H.; Wilson, R. J.; Friend, R. H.; Inbasekaran, M.; Wu, W.; Woo, E. P.; Grell, M.; Bradley, D. D. C. *Appl. Phys. Lett.* **2000**, *77*, 406. (b) Sonar, P.; Singh, S. P.; Sudhakar, S.; Dodabalapur, A.; Sellinger, A. *Chem. Mater.* **2008**, *20*, 3184. (c) Aboubakr, H.; Tamba, M.-G.; Diallo, A. K.; Videlot-Ackermann, C.; Belec, L.; Siri, O.; Raimundo, J.-M.; Mehl, G. H.; Brisset, H. *J. Mater. Chem.* **2012**, *22*, 23159.
(21) Merlo, J. A.; Newman, C. R.; Gerlach, C. P.; Kelley, T. W.; Muyres, D. V.; Fritz, S. E.; Toney, M. F.; Frisbie, C. D. *J. Am. Chem. Soc.* **2005**, *127*, 3997.
(22) Ruiz, R.; Choudhary, D.; Nickel, B.; Toccoli, T.; Chang, K.-C.; Mayer, A. C.; Clancy, P.; Blakely, J. M.; Headrick, R. L.; Iannotta, S.; Malliaras, G. G. *Chem. Mater.* **2004**, *16*, 4497.
(23) Wu, Y.; Li, Y.; Gardner, S.; Ong, B. S. *J. Am. Chem. Soc.* **2005**, *127*, 614.
(24) Carlo, A. D.; Piacenza, F.; Bolognesi, A.; Stadlober, B.; Maresch, H. *Appl. Phys. Lett.* **2005**, *86*, 263501.
(25) Oh, J. H.; Liu, S.; Bao, Z.; Schmidt, R.; Würthner, F. *Appl. Phys. Lett.* **2007**, *91*, 212107.
(26) Gsänger, M.; Oh, J. H.; Könemann, M.; Höffken, H. W.; Krause, A.-M.; Bao, Z.; Würthner, F. *Angew. Chem., Int. Ed.* **2010**, *49*, 740.